Am J Cancer Res 2022;12(5):2173-2188
www.ajcr.us /ISSN:2156-6976/ajcr0142148

*Original Article*

# Nuclear moonlighting of the secreted growth factor heregulin drives endocrine-resistant breast cancer independently of HER2/HER3 signaling

Lin Yang[1], Travis Vander Steen[2], Ingrid Espinoza[3,4], Elisabet Cuyàs[5,6], Sara Verdura[5,6], Javier A Menendez[5,6], Ruth Lupu[2,7,8]

*[1]Precision Cancer Therapeutics Program, Center for Individualized Medicine, Mayo Clinic, Rochester, MN, USA; [2]Department of Laboratory Medicine and Pathology, Division of Experimental Pathology, Mayo Clinic, Rochester, MN, USA; [3]Department of Preventive Medicine, John D. Bower School of Population Health, University of Mississippi Medical Center, Jackson, MS, USA; [4]Cancer Institute, School of Medicine, University of Mississippi Medical Center, Jackson, MS, USA; [5]Program Against Cancer Therapeutic Resistance (ProCURE), Metabolism and Cancer Group, Catalan Institute of Oncology, Girona, Spain; [6]Girona Biomedical Research Institute, Salt, Girona, Spain; [7]Department of Biochemistry and Molecular Biology Laboratory, Mayo Clinic Minnesota, Rochester, MN, USA; [8]Mayo Clinic Cancer Center, Rochester, MN, USA*

Received February 3, 2022; Accepted March 3, 2022; Epub May 15, 2022; Published May 30, 2022

**Abstract:** The HER3/4 ligand heregulin-β2 (HRG) is a secreted growth factor that transactivates the ligand-less receptor HER2 to promote aggressive phenotypes in breast cancer. HRG can also localize to the nucleus of breast cancer cells, but both the nuclear translocation mechanism and the physiological role of nuclear HRG remain elusive. Here we show that nucleolin-driven nuclear moonlighting of HRG uncouples its role as a driver of endocrine resistance from its canonical HER network-activating role in breast cancer. Tandem affinity purification coupled to mass spectrometry identified the intracellular transporter nucleolin as a major HRG-binding protein. HRG interacts with nucleolin via a nuclear localization signal motif located at the N-terminal extracellular domain of HRG. Nucleolin interacts with HRG via aspartate/glutamate-rich acidic stretches located at the N-terminal domain of nucleolin. Depletion of nucleolin abolishes HRG nuclear translocation and decreases HRG mRNA and protein expression. Isolated deficiency of nuclear HRG abolishes the HRG-driven endocrine resistance phenotype *in vitro* and in mouse xenograft models, while preserving its capacity to activate the HRG/HER/MAPK autocrine signaling axis. Conversely, isolated deficiency of secreted HRG to bind HER2/3 receptors does not impair endocrine resistance. The discovery that the functions of dual compartment-resident HRG do not depend on the same effector (i.e., activation of HER2/3 receptors) establishes a new paradigm for the functional and therapeutic relevance of nuclear HRG in breast cancer.

**Keywords:** Heregulin, nucleolin, breast cancer, tamoxifen, endocrine resistance

## Introduction

Heregulin-β2 (HRG) is an archetypal member of a large subclass of secreted growth factors that, through their ability to directly interact with the transmembrane receptors HER3/HER4 and indirectly transactivate HER2, can trigger downstream signaling pathways linked to carcinogenesis, tumor progression, and resistance to cancer therapies [1]. In addition to a cytoplasmic tail and a transmembrane domain, the HRG structure includes a juxtamembrane domain, an EGF-like domain, an immunoglobulin-like domain, and an N-terminus motif, which are all located in the extracellular compartment [2] (**Figure 1A**, *top*). HRG is synthesized as a large membrane-anchored glycosylated precursor that can interact with HER3/HER4 in a juxtacrine fashion via the extracellular EGF-like domain [3]. HRG can be also cleaved from the cellular membrane by metalloproteinases to promote paracrine or autocrine signaling [4]. Binding of HRG to HER3 or HER4 triggers dimerization to HER4 or, preferentially, to the ligand-less receptor HER2, leading to phosphorylation of the intracellular HER domains

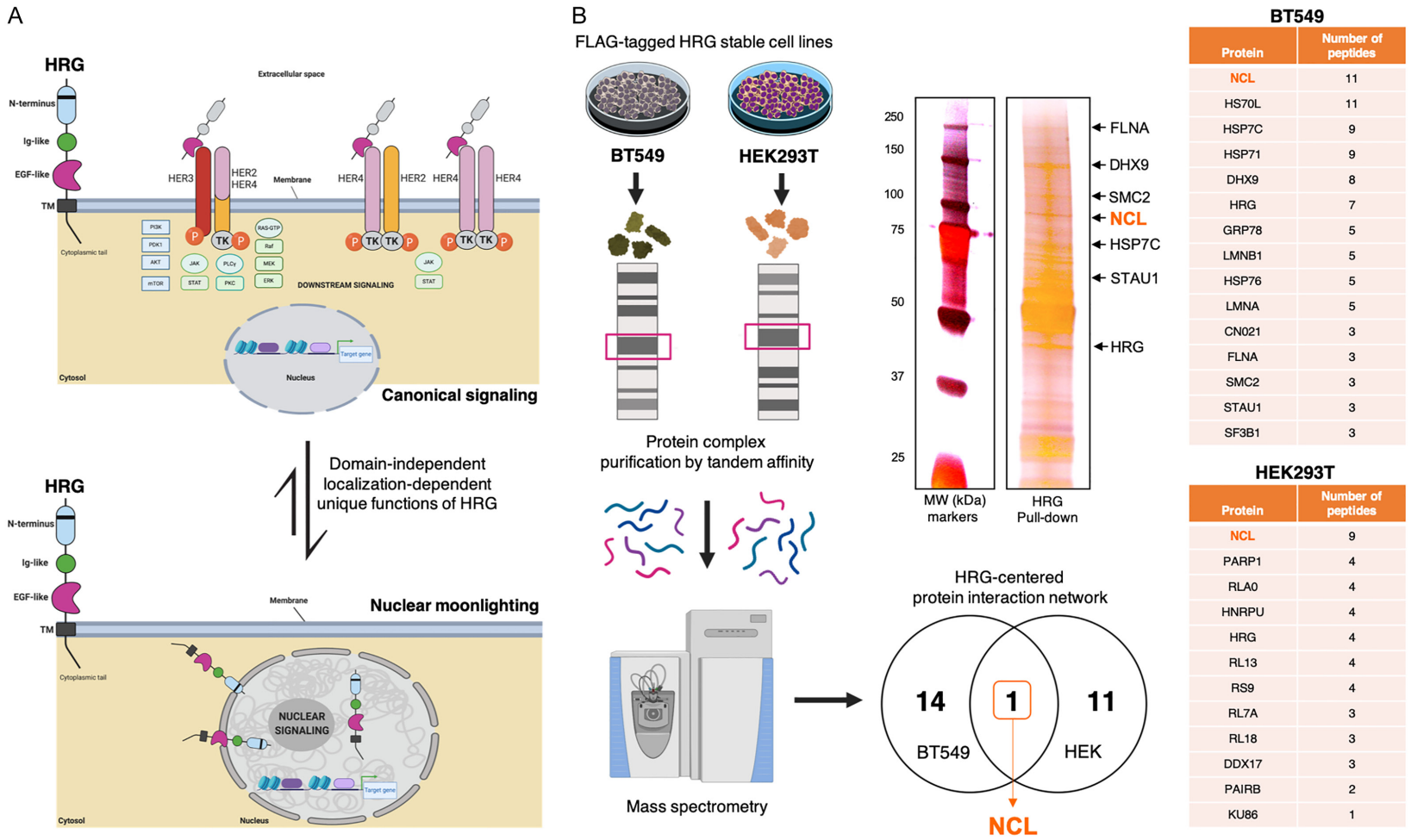


**BT549**

| Protein | Number of peptides |
|---|---|
| NCL | 11 |
| HS70L | 11 |
| HSP7C | 9 |
| HSP71 | 9 |
| DHX9 | 8 |
| HRG | 7 |
| GRP78 | 5 |
| LMNB1 | 5 |
| HSP76 | 5 |
| LMNA | 5 |
| CN021 | 3 |
| FLNA | 3 |
| SMC2 | 3 |
| STAU1 | 3 |
| SF3B1 | 3 |

**HEK293T**

| Protein | Number of peptides |
|---|---|
| NCL | 9 |
| PARP1 | 4 |
| RLA0 | 4 |
| HNRPU | 4 |
| HRG | 4 |
| RL13 | 4 |
| RS9 | 4 |
| RL7A | 3 |
| RL18 | 3 |
| DDX17 | 3 |
| PAIRB | 2 |
| KU86 | 1 |

**Figure 1.** Identification of nucleolin as a major binding partner of heregulin-β2. A. *Top.* Heregulin-β2 (HRG) binds to HER3 and HER4 to mediate downstream signaling linked to breast cancer initiation and progression. HRG binding to HER3 or HER4 triggers dimerization to HER2 or HER4 and phosphorylation of intracellular domains, leading to activation of downstream pathways including MAPK/ERK, PI3K/AKT/mTOR, JAK/STAT, and PKC. *Bottom.* HRG can also localize to the cell nuclei of breast cancer in a HER receptor-independent manner [23]. Although the idea that secretion and subsequent cell surface binding of HER receptors are not prerequisites for HRG nuclear localization, and that non-secreted HRG may function in nuclear compartments has been postulated for more than a decade, both the nuclear translocation mechanisms and the distinct physiological role of nuclear HRG have remained largely elusive. B. Cell lysates prepared from BT549 and HEK293T cells engineered to stably express FLAG-tagged HRG were subjected to protein complex purification by the tandem affinity method. HRG-associated proteins were subsequently separated by one-dimensional SDS/PAGE and visualized by silver staining (inset shows a representative experiment using BT549 cell lysates) prior to mass spectrometry (MS) analysis. Tables summarize the numbers of common peptides and proteins identified by MS. Analysis of the HRG-centered protein interaction network identified nucleolin (NCL), a shuttle protein between the cell surface, cytoplasm, and nucleus, as a major HRG-binding protein.

and activation of downstream pathways (e.g., MAPK/ERK, PI3K/AKT, JAK/STAT, and PKC) [5-8] (**Figure 1A**, *top*). Therefore, the phenotypic outcomes of HRG-driven signaling in human tumors are commonly viewed as the integration of the amount of HRG protein available to bind HER receptors and the predominant type and amount of HER receptors on the cell surface of cancer cells.

Overexpression of HRG in breast cancer cell lines promotes metastatic phenotypes with enhanced motility, increased invasiveness, and hormone-independent cell growth [8-12]. In animal models, HRG overexpression suffices not only to drive mammary gland transformation and proliferation in the presence of hormonal stimulation, but also to induce more aggressive, endocrine therapy-resistant phenotypes with elevated angiogenesis and stemness properties in the absence of estrogen stimulation and independently of HER2 [13]. Selective suppression of HRG by antisense cDNA diminishes tumor formation and growth and prevents metastasis of triple-negative breast cancer cells *in vivo*, supporting the ability of HRG to drive breast cancer progression irrespective of HER2 overexpression [14-16]. Intriguingly, several members of the HRG family can function not only as agonists of HER receptors, but can also reside in the nucleus, where they associate with specific intra-nuclear structures (e.g., nucleoli, nuclear speckles, telomeres) to modify cellular behavior that is not apparently associated with the expression of HER receptors [17-22] (**Figure 1A**, *bottom*). Structural and functional studies with naturally occurring, non-secreted isoforms of HRG lacking a transmembrane domain but harboring a nuclear localization signal (NLS) at the N-terminus (e.g., NRG1-β3), support the notion that secretion and subsequent binding of HRGs to cell surface-associated HER receptors might not be a prerequisite for nuclear localization and functioning in defined nuclear compartments [23-25]. For the more common secreted HRG isoforms, however, it might be argued that the autocrine/paracrine events occurring through engaging their cognate HER receptors cannot be uncoupled from the intra-nuclear intracrine events because all four classes of HER receptors have been found in the nucleus, some of them in association with their ligands [26-31]. Thus, although HRG can localize to the nucleus of cancer cells, both the nuclear translocation mechanism and the physiological role of nuclear HRG remain elusive.

Here, we hypothesized that HRG is a *bona fide* "moonlighting" protein capable of performing a variety of autonomous, physiologically relevant functions without portioning these functions into different protein domains, but rather exclusively depending on its sub-cellular localization (**Figure 1A**, *bottom*). Using a systematic approach that included tandem affinity purification coupled to mass-spectrometry (TAP/MS) to identify HRG-binding candidates that might operate as intra-nuclear transporters of HRG, panels of HRG deletion mutants uniquely lacking in their ability to localize to the nucleus and/or to bind/activate HER receptors, and functional analyses of phenotypic outcomes *in vitro* and in animal models, we unveil that the nucleolin-driven nuclear moonlighting of HRG uncouples its well-known role as a driver of endocrine resistance from its canonical HER receptor-activating role in breast cancer cells.

## Materials and methods

### *Materials*

FLAG/SBP-tagged HRGβ2 was cloned into the pIRES2-EGFP vector. All HRG and nucleolin deletion mutants were generated using the Stratagene QuickChange™ Site-Directed Mutagenesis Kit (La Jolla, CA). Plasmids encoding GFP protein fused with full-length HRG and its NLS-deleted mutant were prepared by cloning HRGβ2 and HRGβ2ΔNLS into the pEGFP-C2 vector (Clontech, Palo Alto, CA).

NCL-GFP was provided by Dr. Kastan at St. Jude Children's Research Hospital (Memphis, TN). Myc-tagged nucleolin was cloned into the pCMV-Tag 3B vector (Stratagene). His-tagged nucleolin was cloned into the pET15b-his vector (Novagen Inc., Madison, WI). Human nucleolin shRNA (sh-NCL-2; TRCN0000062283) targeting the UTR of nucleolin was cloned in the pLKO.1-Puro vector (Sigma-Aldrich, St. Louis, MO).

Monoclonal antibodies against the FLAG epitope (M2) and the Myc epitope (9E10) were purchased from Sigma and Santa Cruz Biotechnology (Santa Cruz, CA), respectively. Rabbit polyclonal anti-HRG (C-20) antibody was pur-

chased from Santa Cruz (sc-348). Mouse monoclonal anti-nucleolin (4E2) antibody was purchased from MBL (Woburn, MA). Rabbit polyclonal anti-NCL antibody was a gift from Dr. Greco at the University of Lyon, France. Mouse monoclonal anti-GST antibody (4C10) and 6 × His tag antibody were purchased from Abcam (Cambridge, UK). Mouse monoclonal anti-ER alpha/NR3A1 antibody was purchased from R&D Systems. (Minneapolis, MN). Rabbit monoclonal anti-HER2/ErbB3 (1B2E) and anti-phospho-HER3/ErbB3 (Tyr1289) (21D3) antibodies were purchased from Cell Signaling Technology, Inc. (Danvers, MA). Goat polyclonal anti-MTA1 antibody (45-094) was purchased from ProSci (Poway, CA).

*Cell culture and transfection*

Human embryonic kidney (HEK) 293T cells and MCF-7 breast cancer cells were grown in Dulbecco's modified Eagle's medium supplemented with 10% fetal bovine serum (FBS, Cellgro®, Mediatech, Inc., Herndon, VA). BT549 breast cancer cells were grown in RPMI 1640 medium supplemented with 10% FBS; MDA-MB-231 cells were grown in IMEM supplemented with 10% FBS. Cells were routinely authenticated to ensure their identity using a short tandem repeat profiling method provided by the Genotyping Shared Resource at Mayo Clinic Rochester. Cells were regularly tested to confirm the absence of mycoplasma using the MycoAlert® Mycoplasma Detection Kit (Lonza, Walkersville, MD). All cell transfections were performed with the GenJet DNA *In Vitro* transfection reagent (SignaGen Laboratories, Rockville, MD).

*Generation of HRG mutants*

The PCR products generated using the HRGβ2 cDNA accession number 183996 (full-length HRGβ2) or the structural deletions mutants ΔNLS, ΔEGF, and ΔNLS + ΔEGF were clones into the retroviral expression vector pBABE-Puro using *Bam*HI and *Eco*RI restriction sites. Retroviral constructs were transfected into a highly efficient amphotropic retroviral TSA54 packaging cell line using FuGENE reagent. For the FuGENE-mediated transfection of full-length HRGβ2 and derivatives, 3.3 μg plasmid DNA of each were added to 330 μL serum-free DMEM followed by the addition of 33 μL FuGENE, in a 1:10 ratio of DNA:FuGENE. After 15 min incubation at room temperature, the solution was added dropwise to MCF-7 cells in a T75 flask containing 10 mL fresh medium. After 48 h of transfection, the retrovirus-containing medium was collected, filtered, and supplemented with Polybrene (Sigma-Chemicals, St. Louis, MO, USA) prior to infection of MCF-7 target cells for an additional 24 h in standard medium. MCF-7/pBABE, MCF-7/HRG, MCF-7/HRGΔNLS, MCF-7/HRGΔEGF, and MCF-7/HRGΔEGF + ΔNLS cells were pooled after 2 days of selection in 2.5 μg/mL puromycin. Alternatively, MCF-7 cells were plated at low density and selected for 1 week in medium containing 2.5 μg/mL puromycin and, after further incubation in the absence of selection, individual colonies were expanded to generate clonal cell lines.

*Purification of HRG-associated proteins*

Cell lysates prepared from BT549 and HEK-293 cells stably expressing FLAG/SBP-tagged HRGβ2 were subjected to immunoprecipitation using anti-FLAG M2 agarose beads (Sigma) followed by S-protein agarose (Novagen). Bound proteins were washed with NETN buffer (20 mmol/L Tris-HCl at pH 8.0, 100 mmol/L NaCl, 1 mmol/L EDTA, and 0.5% Nonidet P-40) three times, boiled in Laemmli buffer, and subjected to SDS/PAGE. Following Coomassie blue staining, the protein bands were excised and subjected to MS analysis to identify specific HRG-associated proteins (Taplin Biology Mass Spectrometry Facility, Harvard Medical School, Boston, MA).

*Purification of 6 × His-tagged NCL from E. coli*

Tagged nucleolin protein was produce recombinant, in BL21 (DE3) cells (Novagen) grown at 37°C until OD = 0.8, then transferred to 18°C and induced with 0.1 mmol/L IPTG for 18 h. The protein was purified using a standard $Ni^{2+}$-NTA protocol.

*Subcellular fractionation*

Subcellular fractions were prepared using the Nuclear Complex Co-IP kit (Active Motif, Carlsbad, CA). The relative purity of each fraction was confirmed by immunoblotting using anti-β-tubulin (cytosolic marker) and anti-PARP1 (nuclear marker) antibodies.

*Immunoprecipitation*

Cells were lysed with NETN buffer containing 50 mmol/L -glycerophosphate, 10 mmol/L NaF, and 1 μg/mL each of pepstatin A, leupeptin, and aprotinin, on ice for 10 min. After removal of cell debris by centrifugation, whole lysates were incubated with the appropriate antibodies in the presence of protein A-protein G (2:1)-agarose beads. Following a wash step with lysis buffer, the immunoprecipitate was subjected to immunoblotting. Detection of antigen-bound antibodies was carried out using the ECL system (Thermo Scientific, Rockford, IL).

*Immunofluorescence*

Cells grown on coverslips were fixed with 3% paraformaldehyde in PBS containing 50 mmol/L sucrose at room temperature for 12 min, washed with PBS three times and permeabilized with 0.2% Triton X-100 in PBS for 15 min. Following permeabilization, slides were washed with 3% non-fat milk three times, and incubated with blocking buffer (supernatant from 3% non-fat milk in PBS) for 15 min. Slides were then incubated with primary antibodies in blocking buffer for 2 h at room temperature. Slides were washed six times with blocking buffer and incubated with secondary antibodies for 1 h, followed by three washes with blocking buffer and three washes with PBS. The slides were fixed again with 3% paraformaldehyde for 5 min and washed three times with PBS. Slides were finally rinsed with milli-Q water, dried, and mounted with Prolong-anti-fade containing DAPI (Molecular Probes/Invitrogen, Eugene, OR). Cells were visualized and imaged using a Zeiss AX10 microscope and a Zeiss LSM510 laser scanning confocal microscope.

*Soft-agar assays*

Cells were grown in phenol red-free IMEM and 5% dextran-coated charcoal-treated bovine serum (CCS) for 5 days in T-75 flasks to deplete estradiol. A bottom layer of 1 mL IMEM containing 0.6% agar and 5% CCS was prepared in 35-mm multi-well cluster dishes. After the bottom layer solidified, cells (20,000/dish) were added in a 1 ml top layer containing either estradiol, tamoxifen, fulvestrant, or combinations thereof, 0.35% Bacto Agar and 5% CCS. Dishes were incubated in a humidified 5% $CO_2$ incubator at 37°C, and colonies measuring ≥ 60 μm were counted after ~12 days using a cell colony counter (Gelcount, Oxford-Optronix, Ltd. Oxford, UK) after staining with nitroblue tetrazolium (Sigma).

*Animal studies*

Xenografts were established by injecting 2 × $10^6$ cells subcutaneously into ovariectomized 3- to -4-week-old athymic female nude-Doxn1$^{nu}$ mice (Harlan Sprague Dawley, Madison, WI) that had been implanted subcutaneously with slow-release estrogen pellets (Innovative Research). When tumors reached a size of approximately 100 $mm^3$, mice bearing MCF-7/pBABE, MCF-7/HRG, MCF-7/HRGΔNLS, MCF-7/HRGΔEGF, and MCF-7/HRGΔEGF + ΔNLS tumors were randomly allocated to continued estrogen treatment or to estrogen withdrawal (by removal of the estrogen pellets) with vehicle alone (untreated group), tamoxifen, or fulvestrant for seven weeks ($n$ = 10 animals/experimental group). Tumor volume was calculated by 3D measurements using the formula: tumor volume ($mm^3$) = (length × width × height)/2. Tumor volume values (mean ± S.D.) were calculated using a Vernier caliper in a blinded manner to minimize experimental bias. Mice were euthanized at completion of the experiment (50 days post-inoculation) or when tumors reached a volume of 1000 $mm^3$, and tumor tissues were removed and maintained at -190°C for later analyses.

*Statistical analysis*

For all experiments, at least three independent experiments were performed with $n \geq 3$ replicate samples per experiment. Investigators were blinded to animal data allocation. Experiments were not randomized. Data are presented as mean ± S.D. Comparisons of means of ≥ 3 groups were performed by one-way ANOVA and Dunnett's t-test for multiple comparisons using GraphPad Prism (GraphPad Software, San Diego, CA, USA). In all studies, $p$-values < 0.05 and < 0.005 were considered to be statistically significant (denoted as * and **, respectively). All statistical tests were two-sided.

## Results

*Nucleolin serves as a major heregulin β2-interacting protein*

To obtain a comprehensive view of the human HRG protein interactome, we adopted a TAP/

MS approach (**Figure 1B**). We employed lysates from HRG-overexpressing BT549 and low-HRG-expressing HEK293T cells stably expressing FLAG-S (2F-2S)-tagged HRG to pull-down binding-partners interacting with HRG. MS analyses of proteins co-purifying with HRG revealed the presence of multiple peptide matches corresponding to various chaperone proteins (e.g., HS70L, HSP7C, HSP71, HSP76, GRP78), nuclear proteins (e.g., FLNA, DHX9, LMNA, SMC2, SF3B1, STAU1, PARP1, HNRPU, DDX17, KU86) and ribosomal proteins (e.g., RLA0, RL13, RS9, RL7A, RL18) (**Figure 1B**). To increase the probability of identifying a functionally relevant HRG-binding protein, we focused on the intracellular transporter nucleolin, the sole shared hit co-immunoprecipitating with HRG in BT549 and HEK293T cells that also showed the highest number of peptide spectrum matches in both cell lines.

Co-immunoprecipitation assays using anti-HRG, anti-nucleolin, and nonspecific IgG antibodies in whole cell extracts from BT549 cells confirmed the interaction between endogenous HRG and nucleolin (**Figure 2A**, *top*). Also, the strong HRG-nucleolin interaction was not detected in immunoblot analyses of immunoprecipitations from HRG- and nucleolin-depleted cells (*data not shown*). *In vitro* approaches confirmed the specific ability of recombinant GST-HRG to bind recombinant poly-histidine-tagged nucleolin expressed in and purified from *Escherichia coli* (**Figure 2A**, *bottom*).

*Heregulin-β2 interacts with nucleolin through a nuclear localization signal motif*

To identify the regions that mediate targeting of HRG to nucleolin, we constructed a series of HRG deletion mutants (**Figure 2B**, *left*). Deletion of the first 97 amino acids comprising the immunoglobulin-like domain and a putative NLS abolished the binding between HRG and nucleolin (**Figure 2B**, *right*). Likewise, the deletion of the predicted bipartite NLS (residues 79-95: RKNKPQNIKIQKKPGKS; **Table 1**) sufficed to fully disrupt the interaction between HRG and nucleolin (**Figure 2C**, *top*). The absence of the NLS motif impeded the nuclear entry and caused cytoplasmic accumulation of HRG (**Figure 2C**, *bottom*). To further confirm whether nuclear localization of HRG was dependent on the putative NLS sequence, we fused GFP to either full-length HRG or an HRG construct lacking this sequence (HRGΔNLS). Transfection of the full-length construct resulted in a diffuse fluorescence signal throughout the cell and nucleus (**Figure 2C**, *right*). Removing the putative NLS resulted in an HRG molecule that was located exclusively outside the nucleus (**Figure 2C**, *right*).

*Nucleolin interacts with heregulin-β2 through the asp/glu-rich N-terminal domain*

To further explore the nature of the HRG-nucleolin interaction, we determined the HRG-binding region of nucleolin in co-immunoprecipitation assays using a series of nucleolin truncation variants (**Figure 2D**, *top*). FLAG-HRG pulled-down full-length nucleolin, central domain mutants lacking each of the RNA recognition motif domains, and a C-terminal mutant lacking the glycine/arginine-rich domain (**Figure 2D**, *bottom*). By contrast, an N-terminal mutant lacking the aspartate/glutamate-rich acidic stretches failed to co-immunoprecipitate with HRG (**Figure 2D**, *bottom*).

*Nucleolin depletion prevents nuclear import of heregulin-β2*

To study the involvement of nucleolin in the naturally occurring nuclear transportation of HRG (**Figure 3A**), we first downregulated its expression using five different short hairpin (sh)RNAs (**Figure 3B**). BT549 cells transiently transfected with nucleolin-shRNA5 showed a decrease in endogenous nucleolin expression of more than 75% (**Figure 3B**). Nucleolin silencing sufficed to drastically prevent the entry of HRG into the nucleus (**Figure 3B**). BT549 cells transduced with a nucleolin-shRNA5 lentivirus similarly exhibited a notable downregulation of HRG at both mRNA and protein levels (**Figure 3B**). Many of the cells displayed a perinucleolar ring phenotype after immunostaining for nucleolin (**Figure 3C**, *white arrows*). HRG was present in the nucleoplasm but was distinctly enriched in speckles close to the nucleolar periphery (**Figure 3C**, *yellow arrows*). Knocking-down nucleolin expression strongly affected the subcellular localization of HRG and its nuclear localization of HRG was completely prevented in nucleolin-silenced cells (**Figure 3C**, *red arrows*).

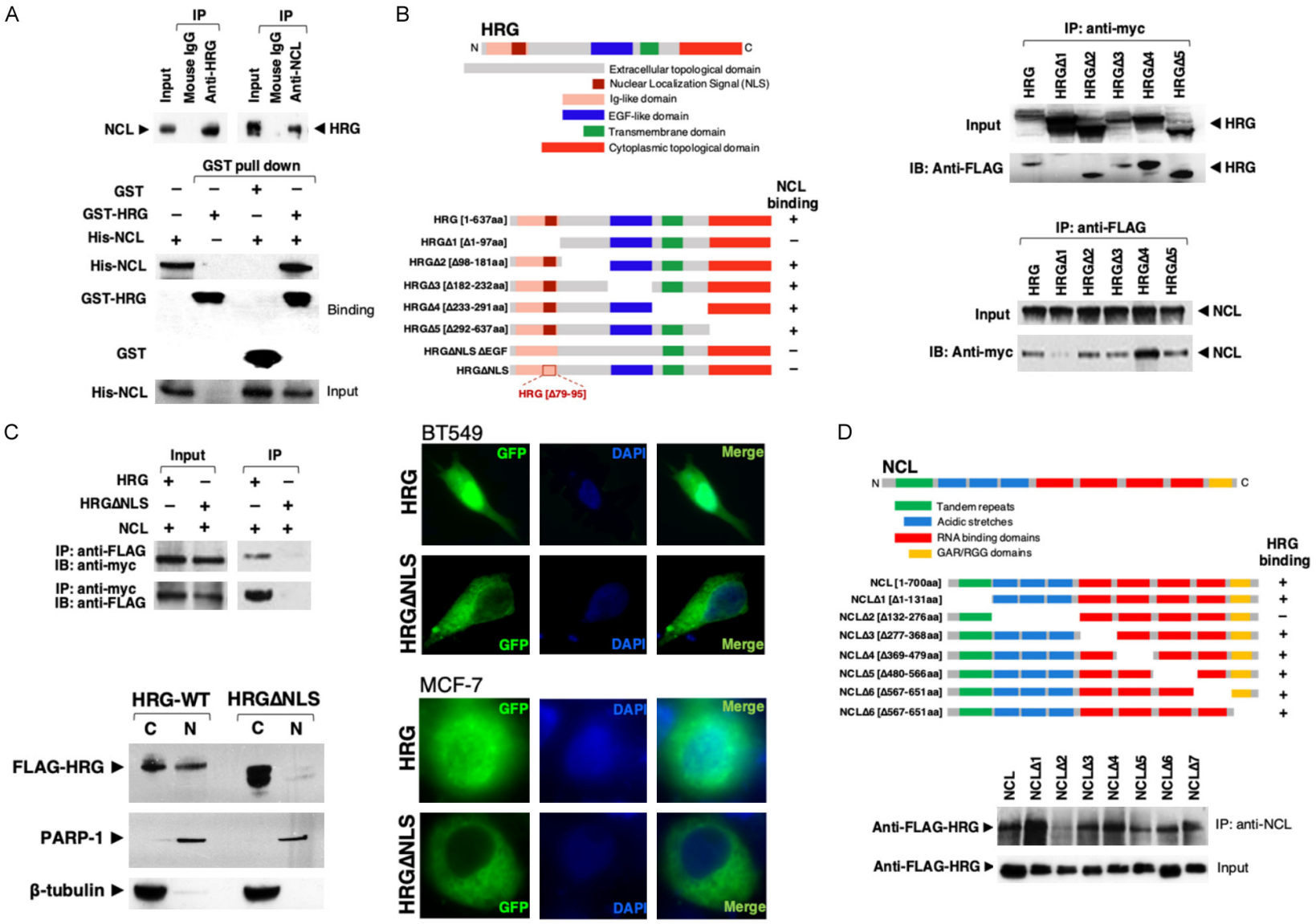


**Figure 2.** Nucleolin interacts with heregulin-β2 *in vitro* and *in vivo*. A. *Top.* Nucleolin (NCL)-heregulin-β2 (HRG) interactions were examined in co-immunoprecipitation (co-IP) assays using BT549 cells. *Bottom.* Representative immunoprecipitation results of *E. coli* BL21 cells expressing His-tagged NCL and GST-HRG using immobilized $Ni^{2+}$. B, C. FLAG-tagged full-length HRG and five deletion mutants of HRG were individually co-transfected with myc-NCL plasmids in HEK293 cells. Myc-tagged NCL in the cell lysates was immunoprecipitated with anti-myc antibodies and immunoblotted with anti-FLAG antibodies. FLAG-tagged HRG in the cell lysates was

immunoprecipitated with anti-FLAG antibodies and immunoblotted with anti-myc antibodies (C = Cytoplasmic extract; N = Nuclear extract). Representative microphotographs show subcellular localization of GFP-tagged full-length HRG and HRG/ΔNLS mutant in BT549 and MCF-7 cells. D. Full-length NCL and seven deletion mutants of NCL were individually co-transfected with FLAG-HRG plasmids in HEK293 cells. Cell lysates were immunoprecipitated with anti-NCL antibodies and immunoblotted with anti-FLAG antibodies.

**Table 1.** Sequences of monopartite and bipartite NLS motifs

| PROTEINS | Sequence |
|---|---|
| Monopartite NLS | |
| SV40 T antigen | PKKKRKV |
| Yeast Histone H2B | GKKRSKV |
| Human c-Myc | PAAKRVKLD |
| Human p53 | PQPKKKP |
| Bipartite NLS | |
| Nucleoplasmin | KRPAATKKAGQAKKKKL |
| Human IL-5 | KKYIDGQKKKCGEERRRVNQ |
| Human RB | KRSAEGSNPPKPLKKLR |
| Human p53 | KRALPNNTSSSPQKKKP |
| Heregulin β2 | RKNKPQNIKIQKKPGKS |

*Deficiency of nuclear heregulin-β2 impedes an endocrine resistance phenotype in vitro*

To evaluate a *bona fide* moonlighting role of nuclear HRG, we tested the hypothesis that prevention of the nucleus-resident function of HRG must lead to impaired phenotypic activity (e.g., endocrine resistance) without altering its canonical HER3-activating role as growth factor in a different cellular compartment. Using estrogen-dependent and antiestrogen-sensitive MCF-7 breast cancer cells as a model, we confirmed that MCF-7 derivatives engineered to stably overexpress full-length HRG (HRG pool and clone HRG-12) became estrogen-independent and antiestrogen-resistant in soft agar colony formation assays [12] (**Figure 4A**). Conversely, MCF-7 derivatives stably overexpressing HRGΔNLS (ΔNLS pool and clone ΔNLS-7) solely exhibited anchorage-independent growth upon supplementation with exogenous estradiol, and were exquisitely sensitive to the growth-inhibitory effects of the anti-estrogens tamoxifen and fulvestrant (ICI 182,780) (**Figure 4A**). Immunoblotting analysis revealed a comparable and strong activation of the HER3/MAPK/ERK pathway in MCF-7/HRG and MCF-7/HRGΔNLS cells (**Figure 4B**). Compared with MCF-7/HRG cells, however, MCF-7/HRGΔNLS cells neither hyper-activated AKT nor downregulated ERα. Metastasis-associated protein 1 (MTA1), a component of the nucleosome remodeling and deacetylase (NuRD) complex that elicits HRG-driven endocrine resistance by repressing ERα transcriptional activity [32, 33], was notably augmented in MCF-7/HRG cells but not in MCF-7/HRGΔNLS cells (**Figure 4B**).

*Nuclear heregulin β2 drives a breast cancer endocrine resistance phenotype in vivo*

To verify the physiological importance of the nuclear moonlighting capacity of HRG, we tested whether the isolated deficiency of nuclear HRG, which preserves its capacity to bind and activate HER receptors via the EGF-like domain, sufficed to abolish HRG-driven endocrine resistance *in vivo*. Using nude mice as an *in vivo* model, we found that transplanted MCF-7/HRGΔNLS cells were fully dependent on estradiol for tumor formation and were exquisitely responsive to tamoxifen and fulvestrant, thus phenotypically mimicking the hormonal-dependency and responsiveness to endocrine therapies of HRG-negative/ER-positive MCF-7/pBABE control cells (**Figure 4C**). We also tested whether the isolated deficiency of secreted HRG to bind HER receptors after specific deletion of the EGF-like domain retained the ability to drive endocrine resistance. MCF-7/HRGΔEGF tumors largely phenocopied the behavior of parental MCF-7/HRG tumors, shown by their estrogen-independent and tamoxifen/fulvestrant-resistant phenotype (**Figure 4C**). Finally, to test for the necessary nuclear localization of the ΔEGF-like derivative of HRG to drive endocrine resistance, we generated a double deletion mutant lacking both the EGF-like domain and the NLS. Prevention of nuclear localization fully suppressed the estrogen-independent and endocrine therapy resistance phenotype of the HER-bindles HRGΔEGF deletion mutant (**Figure 5A**).

## Discussion

HRG is one of many proteins that possesses additional biological activities in cancer cells depending on their subcellular localization [34-

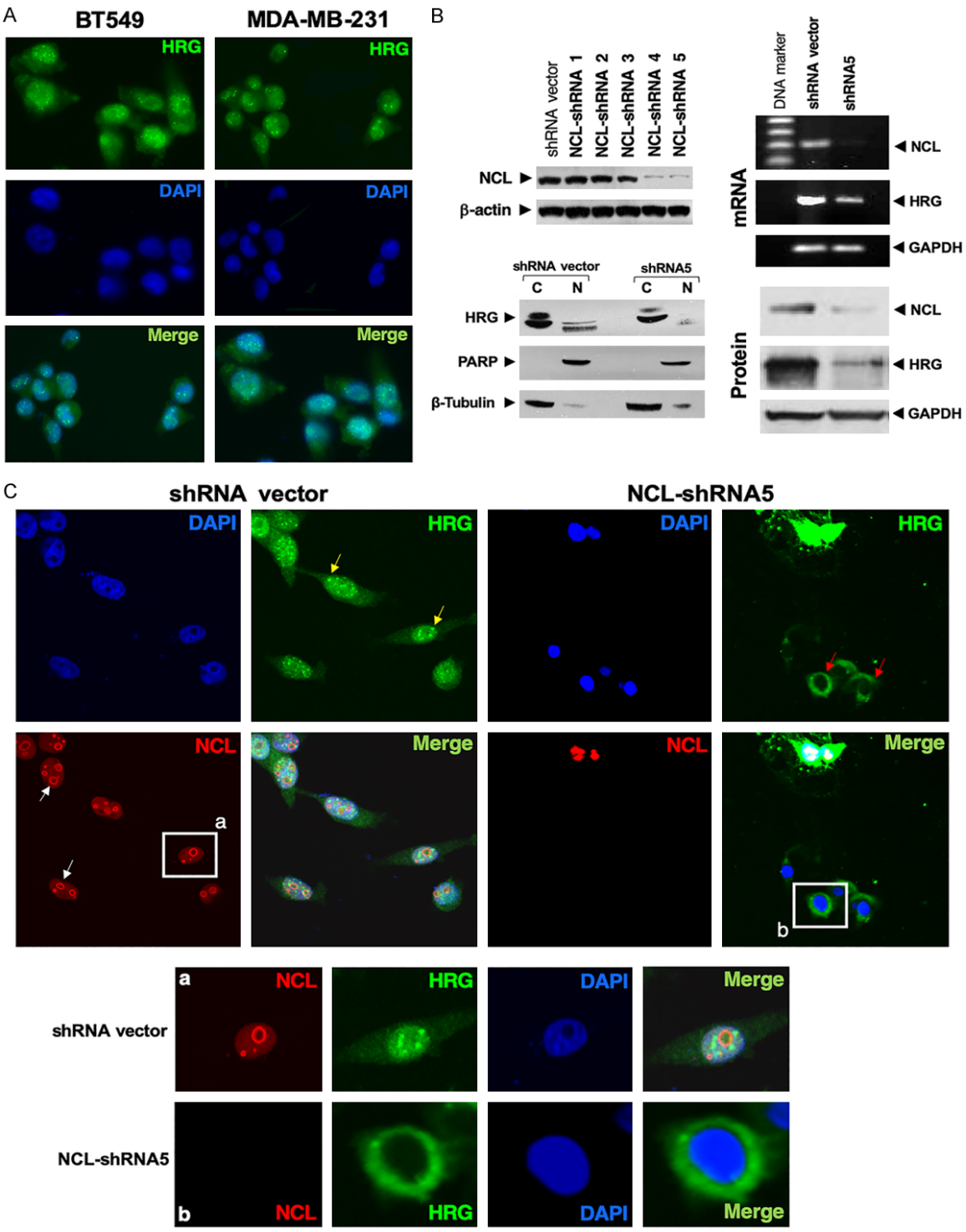


**Figure 3.** Nucleolin drives nuclear shuttling of heregulin-β2. A. Representative microphotographs showing subcellular localization of endogenous HRG in BT549 and MDA-MB-231 cells. B. *Left.* Representative immunoblotting of nucleolin (NCL) expression in BT549 cells transiently transfected with five different NCL-targeting shRNA plasmids. The amount of heregulin-β2 (HRG) in nuclear extracts was examined following transient transfection with a shRNA vector and NCL-targeted shRNA5. Cell lysates were prepared and probed with anti-HRG, β-tubulin (cytosolic marker), and poly-ADP ribose polymerase (PARP, nuclear marker) antibodies. C = cytoplasmic extract, N = nuclear extract. *Right.* Representative results of RT-PCR (*left*) and immunoblotting (*right*) analyses showing the expression of HRG mRNA and protein, respectively, in BT-549 cells stably transduced with shRNA vector and NCL-targeted shRNA5 lentiviruses. C. After transient transfection with a shRNA vector and NCL-targeted shRNA5, BT549 cells were fixed and immunostained using anti-HRG and anti-NCL antibodies; nuclei were labeled with DAPI. The merged images are

also shown. (Yellow arrows: speckled staining of HRG in control cells; white arrows: perinucleolar, ring-like staining of NCL in control cells; red arrows: perinuclear region staining of HRG in NCL-silenced cells). White inserts show high magnification images of representative NCL, HRG, and merged staining patterns.

36]. The best known, canonical mechanism of HRG as a secreted growth factor is to bind HER receptors and propagate signals to intracellular, downstream effectors (**Figure 1A**); however, several isoforms of HRG including HRGβ2 have also been detected in the nucleus, where they might directly perform yet unknown HER receptor-independent regulatory roles (**Figure 1A**). Given the dual location of HRG, an obvious outstanding question is: which of the two compartment-delimited functions of HRG is essential to drive clinically relevant phenotypic traits in cancer? We here provide multiple lines of evidence demonstrating that endocrine resistance is a nucleolin-dependent nuclear moonlighting function of HRG uncoupled from its canonical HER3-activating role in breast cancer (**Figure 5B**, *left*).

Because the ~45 kDa size of HRG is close to the exclusion limit of nuclear pores for passive diffusion into the nucleus, we first sought to identify a mechanism for its nuclear transport. To discriminate putative HRG-transport proteins, we performed TAP/MS of proteins that co-purified with a flagged version of HRG. Co-immunoprecipitation assays verified the interaction between endogenous HRG and nucleolin, a protein capable of associating with specific sets of proteins on the cell surface and in the cytoplasm and nucleoplasm of many cell types [37-43]. We confirmed that HRG contains a bipartite NLS-like motif within its N-terminal region that, although quite different to classical the NLS (**Table 1**), might be accessible to engage in molecular interactions with putative transport factors such as nucleolin. To functionally verify the nucleolin-mediated nuclear import of HRG, we generated a series of HRG mutants, finding that a ΔNLS mutant failed to accumulate in the nucleus in a nucleolin-dependent manner. As a consequence, the HRG/ΔNLS mutant does not bind nucleolin, and depletion of nucleolin effectively prevents HRG nuclear translocation. Thus, failed nuclear targeting of the HRG/ΔNLS mutant is a direct consequence of the abolition of the nucleolin/HRG interaction.

Our data also reveal that the aspartate/glutamate-rich acidic stretches at the N-terminal domain of nucleolin are essential for its interaction with HRG. Intriguingly, the interaction between nucleolin with HRG might be multifunctional, as depletion of nucleolin notably decreased the mRNA and protein expression of HRG. The ability of nucleolin to exert RNA regulatory activity is likely linked to its capacity to associate with target RNAs via the four RNA-binding domains at the central globular domain, and its arginine/glycine-rich C-terminal domain [41, 44]. It is thus tempting to suggest that whereas the nucleolin N-terminal domain drives the shuttling of HRG between the cytoplasmic and nuclear compartments, the ability of the central/C-terminal domains of nucleolin to associate with HRG RNA might augment HRG mRNA stability and translation. Future studies should evaluate whether targeting the RNA-binding activity of nucleolin [45, 46] might reduce its binding to HRG mRNA, resulting in HRG mRNA destabilization and diminished HRG protein levels. We speculate that the intracellular transport of HRG by nucleolin might bring HRG to co-transcriptional active spliceosomes. We previously used the yeast two-hybrid system to search for pairwise interactions between HRGβ2 and interaction partners present in a human mammary gland cDNA library, and reported that one of the HRG-binding candidates was the splicing factor SC35 [22]. In this regard, it is noteworthy that the main component of the splicing machinery, SF3B1, the spliceosome-related RNA helicases DDX17 and DHX9, and the spliceosome factor SMC2-all of them linked also to telomere biology-were included in the HRG-interacting stable interactors predicted by TAP/MS. Nucleolin is part of the breast cancer metastasis-associated perinucleolar compartment [47], where it can co-localize and interact with nuclear speckles that contain SC35 and other proteins primarily implicated in pre-mRNA processing. Although beyond the scope of the present study, identifying which of the many distinct compartments of the nucleus is/are the different sites of HRG nuclear activity (e.g., spliceosome and/or telomere regions) should enrich our understanding of the HRG nuclear functions in cancer cells.

HRG is primarily known for its activating functions on HER receptors. A crucial finding of our

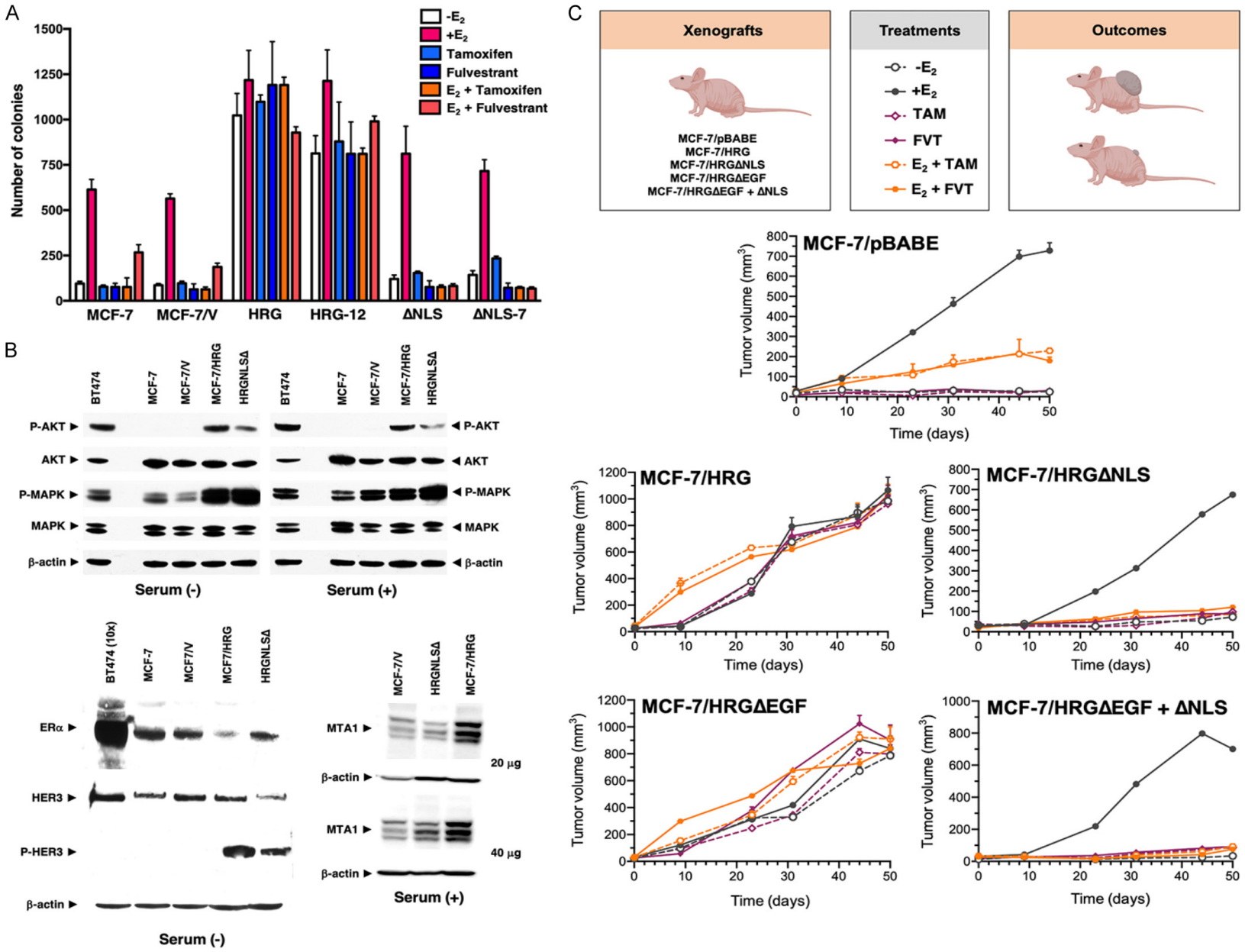
A
Number of colonies
1500
1250
1000
750
500
250
0
-E2
+E2
Tamoxifen
Fulvestrant
E2 + Tamoxifen
E2 + Fulvestrant
MCF-7
MCF-7/V
HRG
HRG-12
ΔNLS
ΔNLS-7
B
BT474
MCF-7
MCF-7/V
MCF-7/HRG
HRGNLSΔ
P-AKT
AKT
P-MAPK
MAPK
β-actin
Serum (-)
Serum (+)
BT474 (10x)
MCF7/V
MCF7/HRG
ERα
HER3
P-HER3
MTA1
20 μg
40 μg
C
Xenografts
MCF-7/pBABE
MCF-7/HRG
MCF-7/HRGΔNLS
MCF-7/HRGΔEGF
MCF-7/HRGΔEGF + ΔNLS
Treatments
-E2
+E2
TAM
FVT
E2 + TAM
E2 + FVT
Outcomes
MCF-7/pBABE
MCF-7/HRG
MCF-7/HRGΔNLS
MCF-7/HRGΔEGF
MCF-7/HRGΔEGF + ΔNLS
Tumor volume (mm3)
Time (days)

**Figure 4.** The isolated deficiency of nuclear heregulin-β2 but not of secreted heregulin-β2 to bind HER receptors abolishes heregulin-β2-driven endocrine resistance *in vitro* and *in vivo*. A. Estradiol ($E_2$)-depleted cells were plated in soft agarose containing $E_2$ ($10^{-9}$ mol/L), tamoxifen ($10^{-7}$ mol/L), fulvestrant ($10^{-7}$ mol/L), their combinations, or ethanol (*v/v*) or DMSO (*v/v*) vehicle only for 7-10 days. Colony formation (≥ 60 μm) was assessed using a colony counter. Each experimental value represents the mean colony number (*columns*) ± S.D. (*bars*) from at least three separate experiments in which triplicate dishes were counted. B. Representative immunoblotting analyses showing the expression of P-HER/total HER, P-AKT/total AKT, P-MAPK/total MAPK, CYR61, ERα, and MTA1, in cells cultured in the absence and presence of serum. C. Shown are the mean tumor volumes (±SD) in MCF-7/pBABE, MCF-7/HRG, MCF-7/HRGΔNLS, MCF-7/HRGΔEGF, and MCF-7/HRGΔEGF + ΔNLS xenograft-bearing nude mice following treatment with estradiol, tamoxifen (TAM), fulvestrant (FVT), or their combinations for seven weeks (n = 10 animals/experimental group).

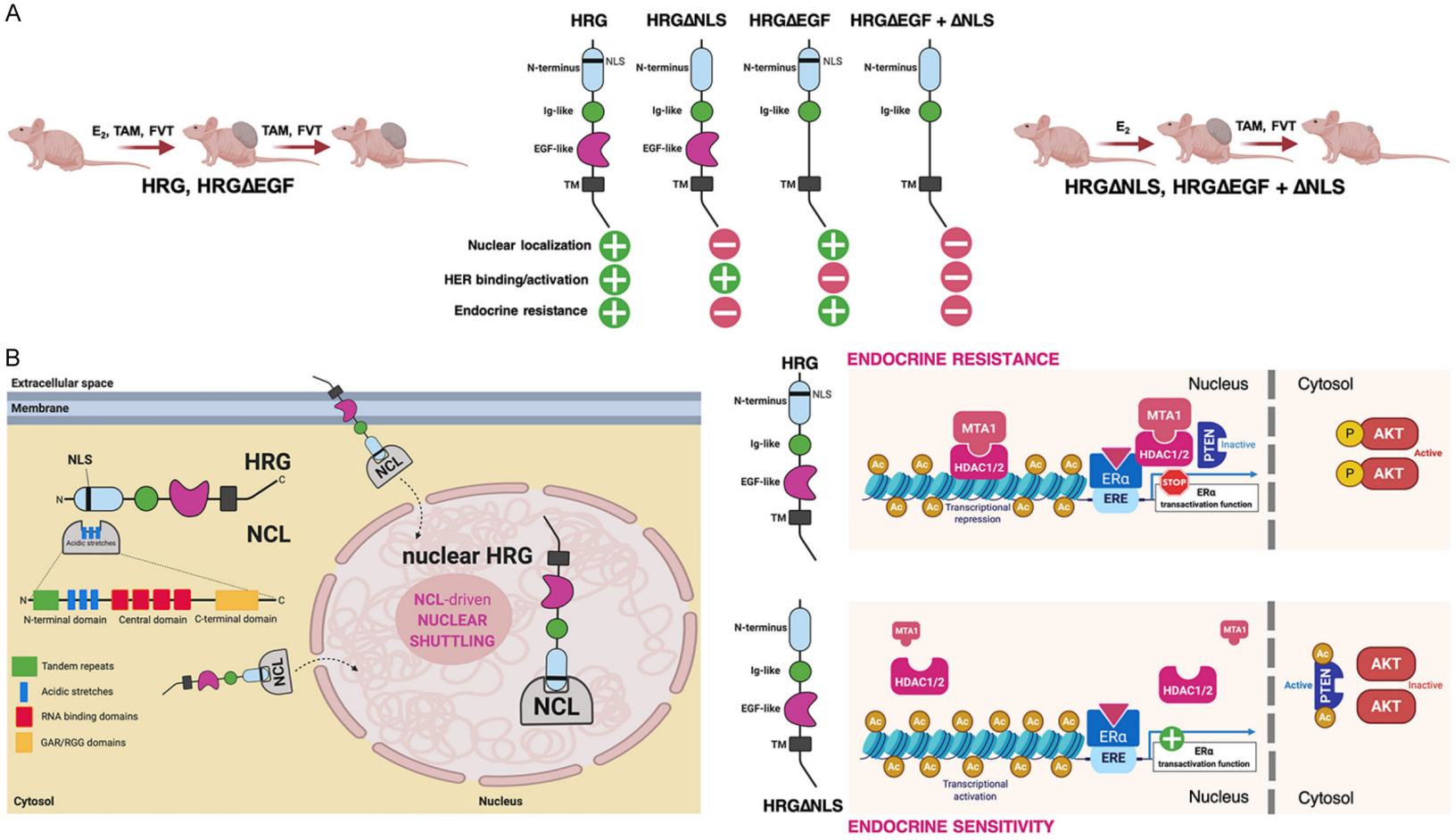

**Figure 5.** Nuclear moonlighting of heregulin-β2 drives endocrine resistance in breast cancer: A working model. A. Isolated deficiency of nuclear HRG abolishes the HRG-driven endocrine resistance phenotype *in vitro* and in mouse xenograft models, while preserving its capacity to activate the HRG/HER/MAPK autocrine signaling axis. Conversely, isolated deficiency of secreted HRG to bind HER receptors does not impair endocrine resistance. B. *Left.* Nucleolin is a/the key driver of HRG nuclear shuttling in breast cancer cells. HRG interacts with nucleolin via a nuclear localization signal motif located at the N-terminal extracellular domain of HRG. Nucleolin interacts with HRG via aspartate/glutamate-rich acidic stretches located at the N-terminal domain of nucleolin. *Right.* MTA proteins (MTA1/2) are part of the chromatin and histone deacetylation complex (NuRD), which contains histone deacetylases (HDAC1/2) and functions in chromatin remodeling and histone deacetylation to drive biologically aggressive cancer phenotypes. MTA1 can directly interact with the ligand-binding domain of the ERα and nuclear HRG can stimulate the association of MTA1 with HDAC2 on the chromatin site of an ER-responsive element (ERE) in the promoter regions of estrogen responsive genes [32]. The repressive function of MTA1 protein on ERα is mediated via histone deacetylation by HDAC1/2, thereby suggesting that nuclear HRG might enhance/stabilize the potent co-repressor epigenetic function of NuRD during the trans-activation of ERα. The MTA1-containing NuRD complex can deacetylate also non-histone proteins such as the tumor-suppressor PTEN. In the presence of nuclear HRG, the MTA1/HDAC complex might be stabilized and localized in the nucleus where it can bind to acetylated PTEN. The MTA1/HDAC complex drives deacetylation (inactivation) of PTEN, which can diffuse into the cytoplasmic compartment but lacking a tumor suppressive function against phospho-active AKT. The isolated deficiency of nuclear HRG suffices to down-regulate MTA1 and disrupt MTA1/HDAC functionality, thereby increasing the acetylated (active) form of PTEN that can then inhibit AKT activity while preserving the HRG capacity to activate the HER/MAPK autocrine signaling axis. The ability of nuclear HRG to drive alterations in acetylation of both histone and non-histone proteins via regulation of the master co-regulatory molecule MTA-1 might explain how the nucleolin-driven nuclear moonlighting of HRG uncouples its well-known role as a driver of endocrine resistance from its canonical HER receptor-activating role in breast cancer cells.

study is that elimination of the EGF-like domain, which is essential and sufficient for HER receptor binding and activation [48], results in a mutant HRG protein that remains fully capable of driving endocrine resistance in breast cancer cells. This indicates that the generally accepted mechanism of action of HRG involving persistent activation of HER receptors does not suffice to drive the endocrine resistance program in estrogen receptor-positive breast cancer cells [49]. Loss of nuclear HRG, however, completely suppresses the signaling events that drive the endocrine resistance phenotype irrespective of the absence/presence of the EGF-like domain (**Figure 5A**). Indeed, the impairment of HRG nuclear moonlighting behaves in a dominant-negative fashion in restoring estrogen dependency and reversing the resistance to tamoxifen and cross-resistance to fulvestrant while fully preserving the capacity of HRG to induce HER2/3 transactivation. Mechanistically, we observed that the previously reported ability of HRG to upregulate MTA1, a component of the NuRD complex that operates as a potent corepressor of estrogen-receptor element-driven transcription, potentially explaining the capacity of HRG to disrupt estrogen responsiveness in breast cancer cells [32, 33], cannot be achieved without the nuclear moonlighting of HRG. It has been reported that when the MTA1/histone deacetylase (HDAC) complex is intact and localized in the nucleus, it operates as an active suppressor unit that binds PTEN-a major negative regulator of PI3K/AKT signaling-to catalyze its deacetylation [50, 51]. Deacetylated-PTEN (enzymatically inactive) not only loses its tumor-suppressive functions in the nucleus, but it can also translocate to the cytoplasm lacking its cytoplasmic lipid phosphatase function, thereby allowing the accumulation of phospho-active AKT (**Figure 5B**, *right*). Inhibition of MTA1 and loss of the MTA1/HDAC complex functionality allows the accumulation of "free" acetylated PTEN with enhanced lipid phosphatase activity, thereby eliciting its tumor-suppressive function in the nucleus and resulting in the repression of AKT activity in the cytoplasm [50, 51]. This model provides a biochemical mechanism through which the loss of the nuclear signaling branch of HRG can differentially prevent AKT activation without altering MAPK activation, which likely relies on the HER-dependent cytosolic signaling branch of HRG. While the precise molecular mechanism(s) underlying the capacity of nuclear HRG to deactivate the MTA1/HDAC complex remain obscure, our results support a plausible mechanism by which nuclear HRG, by reversing pathological epigenetic changes mediated by the co-repressor MTA1/HDAC complex (**Figure 5**, *right*), can exert repressive functions on both ERα transactivation and AKT signaling to autonomously drive endocrine resistance in breast cancer without the participation of HER receptors.

In summary, our study reveals that there is considerably more complexity than previously appreciated in how HRG signaling is constructed in cancer cells to pattern a compartment-specific functional outcome. The discovery that the functions of dual compartment-resident HRG do not depend on the same effectors (i.e., activation of HER receptors) might help to establish a new paradigm for the physiological role and therapeutic relevance of nuclear HRGs during breast cancer progression. Clarifying the molecular basis of how the nuclear moonlighting of HRG involving not only its nucleolin-dependent active transport to the cell nucleus, but also its likely association with and regulation of nuclear proteins and/or target genes (**Figure 5**), will shed further light on the non-HER receptor-related functions of other HRG isoforms in their regulation of nuclear functions of cell-fate choices in both normal and pathological processes.

## Acknowledgements

This work was supported by the NIH National Cancer Institute Grants R01 CA116623 (to Ruth Lupu) and by the U.S. Department of Defense (DOD)-Breakthrough 3 Grants BC15-1072 and BC151072P1 (to Ruth Lupu). Work in the Menendez laboratory is supported by the Spanish Ministry of Science and Innovation (Grant PID2019-10455GB-I00, Plan Nacional de I+D+I, founded by the European Regional Development Fund, Spain) and by an unrestricted research grant from the Fundació Oncolliga Girona (Lliga catalana d'ajuda al malalt de càncer, Girona). Elisabet Cuyàs is a recipient of a "Miguel Servet" research contract (CP20/00003) from the Instituto de Salud Carlos III, Spanish Ministry of Science and Innovation (Spain). The authors would like to thank Dr. Kenneth McCreath for editorial support.

## Disclosure of conflict of interest

None.

**Address correspondence to:** Ruth Lupu, Mayo Clinic, Department of Experimental Pathology, 200 First Street SW, Rochester 55905, MN, USA. E-mail: lupu.ruth@mayo.edu; Javier A Menendez, Catalan Institute of Oncology (ICO), Girona Biomedical Research Institute (IDIBGI), Edifici M2, Parc Hospitalari Martí i Julià, Salt E-17190, Girona, Spain. E-mail: jmenendez@idibgi.org

## References

[1] Meyer D, Yamaai T, Garratt A, Riethmacher-Sonnenberg E, Kane D, Theill LE and Birchmeier C. Isoform-specific expression and function of neuregulin. Development 1997; 124: 3575-3586.

[2] Barbacci EG, Guarino BC, Stroh JG, Singleton DH, Rosnack KJ, Moyer JD and Andrews GC. The structural basis for the specificity of epidermal growth factor and heregulin binding. J Biol Chem 1995; 270: 9585-9589.

[3] Burgess TL, Ross SL, Qian YX, Brankow D and Hu S. Biosynthetic processing of neu differentiation factor. Glycosylation trafficking, and regulated cleavage from the cell surface. J Biol Chem 1995; 270: 19188-19196.

[4] Zhou BB, Peyton M, He B, Liu C, Girard L, Caudler E, Lo Y, Baribaud F, Mikami I, Reguart N, Yang G, Li Y, Yao W, Vaddi K, Gazdar AF, Friedman SM, Jablons DM, Newton RC, Fridman JS, Minna JD and Scherle PA. Targeting ADAM-mediated ligand cleavage to inhibit HER3 and EGFR pathways in non-small cell lung cancer. Cancer Cell 2006; 10: 39-50.

[5] Montero JC, Rodríguez-Barrueco R, Ocaña A, Díaz-Rodríguez E, Esparís-Ogando A and Pandiella A. Neuregulins and cancer. Clin Cancer Res 2008; 14: 3237-3241.

[6] Montero JC, Rodríguez-Barrueco R and Pandiella A. Transautocrine signaling by membrane neuregulins requires cell surface targeting, which is controlled by multiple domains. J Biol Chem 2011; 286: 24350-24363.

[7] Centa A, Rodríguez-Barrueco R, Montero JC and Pandiella A. The immunoglobulin-like domain of neuregulins potentiates ErbB3/HER3 activation and cellular proliferation. Mol Oncol 2018; 12: 1061-1076.

[8] Mota JM, Collier KA, Barros Costa RL, Taxter T, Kalyan A, Leite CA, Chae YK, Giles FJ and Carneiro BA. A comprehensive review of heregulins, HER3, and HER4 as potential therapeutic targets in cancer. Oncotarget 2017; 8: 89284-89306.

[9] Lupu R, Cardillo M, Cho C, Harris L, Hijazi M, Perez C, Rosenberg K, Yang D and Tang C. The significance of heregulin in breast cancer tumor progression and drug resistance. Breast Cancer Res Treat 1996; 38: 57-66.

[10] Hijazi MM, Thompson EW, Tang C, Coopman P, Torri JA, Yang D, Mueller SC and Lupu R. Heregulin regulates the actin cytoskeleton and promotes invasive properties in breast cancer cell lines. Int J Oncol 2000; 17: 629-641.

[11] Grunt TW, Saceda M, Martin MB, Lupu R, Dittrich E, Krupitza G, Harant H, Huber H and Dittrich C. Bidirectional interactions between the estrogen receptor and the cerbB-2 signal-

ing pathways: heregulin inhibits estrogenic effects in breast cancer cells. Int J Cancer 1995; 63: 560-567.
[12] Tang CK, Perez C, Grunt T, Waibel C, Cho C and Lupu R. Involvement of heregulin-beta2 in the acquisition of the hormone-independent phenotype of breast cancer cells. Cancer Res 1996; 56: 3350-3358.
[13] Atlas E, Cardillo M, Mehmi I, Zahedkargaran H, Tang C and Lupu R. Heregulin is sufficient for the promotion of tumorigenicity and metastasis of breast cancer cells in vivo. Mol Cancer Res 2003; 1: 165-175.
[14] Tsai MS, Shamon-Taylor LA, Mehmi I, Tang CK and Lupu R. Blockage of heregulin expression inhibits tumorigenicity and metastasis of breast cancer. Oncogene 2003; 22: 761-768.
[15] Atlas E, Bojanowski K, Mehmi I and Lupu R. A deletion mutant of heregulin increases the sensitivity of breast cancer cells to chemotherapy without promoting tumorigenicity. Oncogene 2003; 22: 3441-3451.
[16] Khurana A, Gonzalez-Guerrico A and Lupu R. Heregulin in breast cancer: old story, new paradigm. Curr Pharm Des 2014; 20: 4874-4878.
[17] Li W, Park JW, Nuijens A, Sliwkowski MX and Keller GA. Heregulin is rapidly translocated to the nucleus and its transport is correlated with c-myc induction in breast cancer cells. Oncogene 1996; 12: 2473-2477.
[18] Fluge O, Akslen LA, Haugen DR, Varhaug JE and Lillehaug JR. Expression of heregulins and associations with the ErbB family of tyrosine kinase receptors in papillary thyroid carcinomas. Int J Cancer 2000; 87: 763-770.
[19] Gilbertson RJ, Clifford SC, MacMeekin W, Meekin W, Wright C, Perry RH, Kelly P, Pearson AD and Lunec J. Expression of the ErbB-neuregulin signaling network during human cerebellar development: implications for the biology of medulloblastoma. Cancer Res 1998; 58: 3932-3941.
[20] Marshall C, Blackburn E, Clark M, Humphreys S and Gullick WJ. Neuregulins 1-4 are expressed in the cytoplasm or nuclei of ductal carcinoma (in situ) of the human breast. Breast Cancer Res Treat 2006; 96: 163-168.
[21] Menendez JA, Rubio MA, Campisi J and Lupu R. Heregulin, a new regulator of telomere length in human cells. Oncotarget 2015; 6: 39422-39436.
[22] Menendez JA, Benboudjema L, Vellon L, Rubio MA, Espinoza I, Campisi J and Lupu R. Heregulin, a new interactor of the telosome/shelterin complex in human telomeres. Oncotarget 2015; 6: 39408-39421.
[23] Golding M, Ruhrberg C, Sandle J and Gullick WJ. Mapping nucleolar and spliceosome localization sequences of neuregulin1-beta3. Exp Cell Res 2004; 299: 110-118.
[24] Hayes NV and Gullick WJ. The neuregulin family of genes and their multiple splice variants in breast cancer. J Mammary Gland Biol Neoplasia 2008; 13: 205-214.
[25] Wang M, Trim CM and Gullick WJ. Localization of Neuregulin 1-β3 to different sub-nuclear structures alters gene expression. Exp Cell Res 2011; 317: 423-432.
[26] Brand TM, Iida M, Corrigan KL, Braverman CM, Coan JP, Flanigan BG, Stein AP, Salgia R, Rolff J, Kimple RJ and Wheeler DL. The receptor tyrosine kinase AXL mediates nuclear translocation of the epidermal growth factor receptor. Sci Signal 2017; 10: eaag1064.
[27] Redmond AM, Omarjee S, Chernukhin I, Le Romancer M and Carroll JS. Analysis of HER2 genomic binding in breast cancer cells identifies a global role in direct gene regulation. PLoS One 2019; 14: e0225180.
[28] Wang SC, Lien HC, Xia W, Chen IF, Lo HW, Wang Z, Ali-Seyed M, Lee DF, Bartholomeusz G, Ou-Yang F, Giri DK and Hung MC. Binding at and transactivation of the COX-2 promoter by nuclear tyrosine kinase receptor ErbB-2. Cancer Cell 2004; 6: 251-261.
[29] Mohd Nafi SN, Generali D, Kramer-Marek G, Gijsen M, Strina C, Cappelletti M, Andreis D, Haider S, Li JL, Bridges E, Capala J, Ioannis R, Harris AL and Kong A. Nuclear HER4 mediates acquired resistance to trastuzumab and is associated with poor outcome in HER2 positive breast cancer. Oncotarget 2014; 5: 5934-5949.
[30] Brand TM, Iida M, Luthar N, Wleklinski MJ, Starr MM and Wheeler DL. Mapping C-terminal transactivation domains of the nuclear HER family receptor tyrosine kinase HER3. PLoS One 2013; 8: e71518.
[31] Lin SY, Makino K, Xia W, Matin A, Wen Y, Kwong KY, Bourguignon L and Hung MC. Nuclear localization of EGF receptor and its potential new role as a transcription factor. Nat Cell Biol 2001; 3: 802-808.
[32] Mazumdar A, Wang RA, Mishra SK, Adam L, Bagheri-Yarmand R, Mandal M, Vadlamudi RK and Kumar R. Transcriptional repression of oestrogen receptor by metastasis-associated protein 1 corepressor. Nat Cell Biol 2001; 3: 30-37.
[33] Manavathi B, Singh K and Kumar R. MTA family of coregulators in nuclear receptor biology and pathology. Nucl Recept Signal 2007; 5: e010.
[34] Monaghan RM and Whitmarsh AJ. Mitochondrial proteins moonlighting in the nucleus. Trends Biochem Sci 2015; 40: 728-735.

[35] Boukouris AE, Zervopoulos SD and Michelakis ED. Metabolic enzymes moonlighting in the nucleus: metabolic regulation of gene transcription. Trends Biochem Sci 2016; 41: 712-730.
[36] Min KW, Lee SH and Baek SJ. Moonlighting proteins in cancer. Cancer Lett 2016; 370: 108-116.
[37] Ginisty H, Sicard H, Roger B and Bouvet P. Structure and functions of nucleolin. J Cell Sci 1999; 112: 761-772.
[38] Cong C, Das S and Bouvet P. The multiple properties and functions of nucleolin. In: The Nucleolus, Protein Reviews Series, Atassi M.Z., editors. New York, NY, USA: Springer; 2011. pp. 185.
[39] Jeffery CJ. An introduction to protein moonlighting. Biochem Soc Trans 2014; 42: 1679-1683.
[40] Berger CM, Gaume X and Bouvet P. The roles of nucleolin subcellular localization in cancer. Biochimie 2015; 113: 78-85.
[41] Jia W, Yao Z, Zhao J, Guan Q and Gao L. New perspectives of physiological and pathological functions of nucleolin (NCL). Life Sci 2017; 186: 1-10.
[42] Ugrinova I, Petrova M, Chalabi-Dchar M and Bouvet P. Multifaceted nucleolin protein and its molecular partners in oncogenesis. Adv Protein Chem Struct Biol 2018; 111: 133-164.
[43] Ugrinova I, Chalabi-Dchar M, Monier K and Bouvet P. Nucleolin interacts and co-localizes with component of pre-catalytic spliceosome complexes. Science 2019; 1: 33.
[44] Abdelmohsen K and Gorospe M. RNA-binding protein nucleolin in disease. RNA Biol 2012; 9: 799-808.
[45] Hanakahi LA, Sun H and Maizels N. High affinity interactions of nucleolin with G-G-paired rDNA. J Biol Chem 1999; 274: 15908-15912.
[46] Soundararajan S, Chen W, Spicer EK, Courtenay-Luck N and Fernandes DJ. The nucleolin targeting aptamer AS1411 destabilizes Bcl-2 messenger RNA in human breast cancer cells. Cancer Res 2008; 68: 2358-2365.
[47] Kamath RV, Thor AD, Wang C, Edgerton SM, Slusarczyk A, Leary DJ, Wang J, Wiley EL, Jovanovic B, Wu Q, Nayar R, Kovarik P, Shi F and Huang S. Perinucleolar compartment prevalence has an independent prognostic value for breast cancer. Cancer Res 2005; 65: 246-253.
[48] Weinstein EJ and Leder P. The extracellular region of heregulin is sufficient to promote mammary gland proliferation and tumorigenesis but not apoptosis. Cancer Res 2000; 60: 3856-3861.
[49] Loi S, Sotiriou C, Haibe-Kains B, Lallemand F, Conus NM, Piccart MJ, Speed TP and McArthur GA. Gene expression profiling identifies activated growth factor signaling in poor prognosis (Luminal-B) estrogen receptor positive breast cancer. BMC Med Genomics 2009; 2: 37.
[50] Dhar S, Kumar A, Li K, Tzivion G and Levenson AS. Resveratrol regulates PTEN/Akt pathway through inhibition of MTA1/HDAC unit of the NuRD complex in prostate cancer. Biochim Biophys Acta 2015; 1853: 265-275.
[51] Qian YY, Liu ZS, Yan HJ, Yuan YF, Levenson AS and Li K. Pterostilbene inhibits MTA1/HDAC1 complex leading to PTEN acetylation in hepatocellular carcinoma. Biomed Pharmacother 2018; 101: 852-859.